Dynamics of Pin Electrode in Pin-to-Plate Discharge System

Hiroyuki Kawamoto, Kosuke Takasaki and Hiromu Yasuda
Department of Mechanical Engineering, Waseda University
Shinjuku, Tokyo, Japan

Abstract

The following singular phenomena were observed on dynamics of a pin electrode in a pin-to-plate gas discharge system. (1) When the axial stiffness of the support of the pin electrode was low, vibration of the pin electrode perpendicular to the plate electrode was observed at the transition from the dark discharge to the corona discharge. (2) A spark-coupled-vibration took place for the softly supported pin electrode at the spark discharge. (3) An electrostatic ink jet phenomenon was observed, when an insulative capillary tube filled with ink was used for the pin electrode. (4) On the contrary, when the plate electrode made of metal was replaced to water, repulsive reaction due to the corona wind changed the shape of water level. (5) When the flexural rigidity of the pin electrode was extremely low, unstable vibration of the pin electrode, flutter, took place at the corona discharge due to the ionic wind. These phenomena are expected to be utilized for a new ozone free charger, a new ink jet system, and a driving system of a micromachine. In addition to these applications, the clarification of the dynamics is indispensable to improve the bead-carry-out in the two-component magnetic blush development subsystem of electrophotography.

Introduction

Electrostatics of a pin-to-plate discharge system has been widely investigated mainly in the field of the high voltage engineering. However, no systematic study has been conducted for kinetics of the pin-to-plate system except for the measurement of corona-induced force per hanging water drop from a high voltage transmission line and ionic wind in the mechanism of corona induced vibration.[1] The authors have studied dynamics of the system, because it is an important basis for the following applications related to the imaging technology.

The first application is a new ozone-free charger of electrophotography under development. It has pin electrodes to which DC high voltage is applied through each resistor. It was confirmed that interposed resistors control sway and dispersion of discharge current from each discharge electrode.[2,3] Consequently it uniformly charges the photoreceptor with less discharge current and an amount of generated ozone is less than that of the former charging device with parallel-connected saw-tooth electrodes to which high voltage is directly applied. Kawamoto[4] has established a theoretical model to calculate ozone emission from this new device. Results of the calculation were compared with experimental results and feasibility for the electrophotography charger was discussed. It was cited that the pin charger has a potential to realize virtually ozone-free. However, several subjects to be overcome still exist to put the charger to practical use. Statics and dynamics of the discharge electrode are the other issues of this charger, especially in the case that the stiffness of the discharge electrode is low. The electrode is deformed and/or the electrostatic force induces abnormal vibration. This is also the case when a blush or magnetic bead chains are used as pin electrodes to realize a cleaner-less system.

The second application is a clarification of a "bead carry-out" phenomenon in electrophotography.[5] A magnetic blush development subsystem in electrophotography is assumed the pin-to-plate system; a bead chain corresponds to the pin and the photoconductor is the plate electrode. If carrier beads escape from a developer sleeve and adhere to the photoconductor surface, they cause serious image defects. Although many kinds of forces, such as magnetic, centrifugal, and Van der Waals, are related to the separation of carrier beads from the chain, the electrostatic force is one of major factors. The present work is utilized to the clarification of this phenomenon called "bead carry-out."

The third application is related to an ink-jet system. When an insulative capillary tube filled with ink was used for the pin electrode, an electrostatic ink jet phenomenon was observed. A preliminary research was also performed on this phenomenon.

The forth is not for the imaging technology but for a driving system of a micromachine. Although force induced in the pin-to-plate discharge system is extremely small, it is large enough to drive micromachines. A new concept that utilizes a piezoelectric element is under investigation.

Electrostatic Force and Electrode Vibration

Fundamental Characteristics

The voltage-current relationship and the electrostatic force in the pin-to-plate system have been already reported.[6] However, because the present study is constructed on the basis of the corona and spark discharge in the pin-to-plate

system, essence of the former investigation is summarized in this section.

Experimental. Because the electrostatic force applied to the pin electrode is extremely small, an experimental set-up shown in Figure 1 was constructed. A wire made of stainless steel was hung down perpendicular to a steel plate. It was connected to the free end of the cantilever plate made of stainless steel. The displacement at the free end of the cantilever was measured by a laser displacement meter (Keyence Corp., LK-2000) and the electrostatic force to the pin was derived multiplying the measured displacement and the stiffness of the cantilever. Two plates were prepared; low stiffness (0.377 N/m) and relatively high stiffness (2.31 N/m). The former was used to measure extremely low force observed at low applied voltage and the later was for the measurement of relatively large force at corona discharge. The stiffness was statically measured dividing weights put on the free end of the plate by the static displacement measured by the laser displacement meter. Because the axial electrostatic force to the pin was less than 0.034 gram at the corona discharging and hence the axial displacement of the pin was less than 0.17 mm, change of the gap during the corona discharging was negligible compared with the air gap, larger than 3.0 mm. Gap between the pin and the plate was adjusted using a mechanical stage attached at the back of the plate electrode. High voltage was applied to the gap by a DC power supply (Matsusada Precision Inc., HVR-10P (positive) and HVR-10N (negative), 0 ~ ±10 kV adjustable, maximum current 0.15 mA). Voltage was determined by a potentiometer of the power supply and current was measured by the voltage drop in a current-shunt resistor. The surface of electrodes was frequently polished to prevent oxidation and chemical deposition on the tip of the discharge electrode due to gas discharge. Reproducibility of data was confirmed during experiments.

A series of experiment was conducted to measure the voltage-current relationship and the electrostatic force. Parameters of the experiment were the pin diameter, 0.2, 0.3, 0.4, 0.5 mm, and the air gap in the range of 3-8 mm.

Voltage-Current Relationship. Figure 2 shows an example of measured voltage-current characteristics. Fundamental features were similar with those of a corotron.[5] At the voltage lower than the threshold (2-3 kV), no substantial current flowed in the air gap. However, over the threshold voltage, discharge current in the order of several microamperes was measured and at the same time weak luminescence was observed at the tip of the pin electrode. That is, the corona discharge took place. The current and luminescence were stable and the discharge was silent. If the applied voltage was more increased, the corona discharge shifted to the spark discharge. Because the spark discharge is non-selfsustaining, the discharge was not continuous but intermittent. Since the current was restricted by the capacity of the power supply, the arc discharge did not take place.

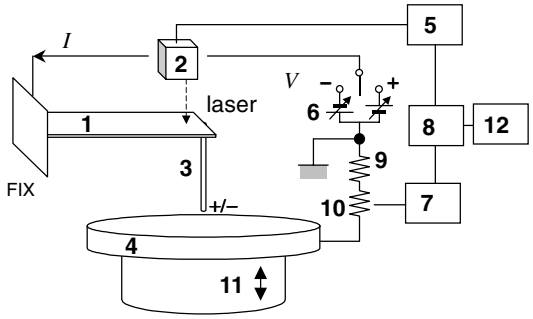

Figure 1. Experimental set-up. (1: stainless steel plate, cantilever, (1) low stiffness T0.1/L140/W10 mm, (2) high stiffness T0.1/L100/ W20 mm, 2: laser sensor, 3: pin electrode, stainless steel, ϕ 0.2-0.5 mm, 4: plate electrode, steel, 5: laser displacement meter, 6: DC high voltage power supply, 7: DC volt meter, 8: oscilloscope, 9: resistor, 500 kΩ, 10: shunt resistor, 3 kΩ, 11: mechanical stage, 12: FFT Analyzer)

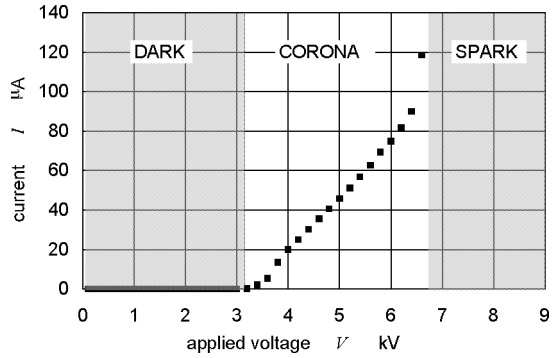

Figure 2. V-I curve in pin-to plate system. (positive, ϕ 0.5 mm pin diameter, 5 mm air gap)

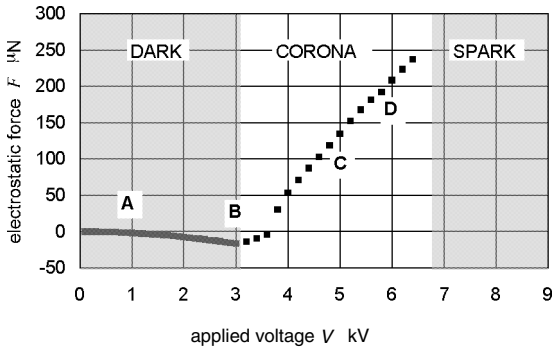

Figure 3. Force applied to pin electrode in pin-to plate system. (positive, ϕ 0.5 mm pin diameter, 5 mm air gap)

Electrostatic Force. Figure 3 is an example of the measured electrostatic force to the pin electrode. Experimental conditions are the same with those of Figure 2. The force acts to the vertical direction and the force applied to the upper direction is designated to be positive. Even at the voltage lower than the threshold, small electrostatic *attractive* force was induced. It was only in the order of 10 μN. The force is proportional to a square of the

voltage and independent of positive or negative. Over the threshold voltage, the force was *repulsive* and became large, in the order of 100 μN, in accordance with the increase of voltage. It showed little dependence to the air gap, the pin diameter, and the difference of positive or negative corona. Preliminary experiment to visualize airflow in the vicinity of the pin electrode suggested that convection of air, ionic wind, is the cause of the repulsive force at corona discharge. This assumption was confirmed by separate experiments shown in succeeding sections. Although the force was very small, it is large enough to change the form of the blush or magnetic bead chains and it is large in more than two orders of magnitude compared with the magnetic force to carrier beads in the magnetic development subsystem (in the order of 0.1-1 μN). The electrostatic force is one of the most important factors that affect the bead carry-out.

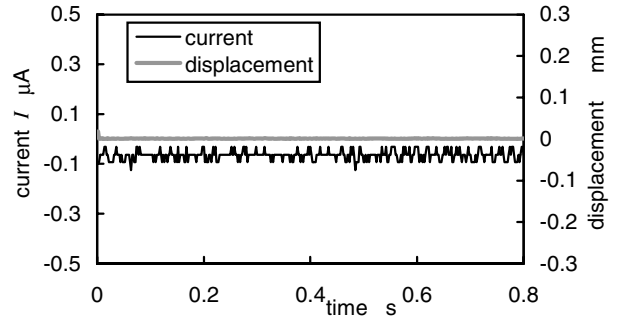

Figure 4. Vertical displacement of pin electrode and discharge current. (1 kV, positive, ϕ 0.5 mm pin diameter, 5 mm air gap)

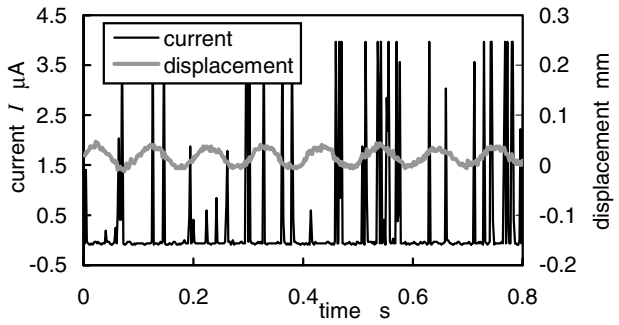

Figure 5. Vertical displacement of pin electrode and discharge current. (3 kV, positive, ϕ 0.5 mm pin diameter, 5 mm air gap)

Vibration of Pin Electrode at Corona Discharge

Because the electrostatic force at the dark and corona discharge is static, it is expected that the force induces only static displacement of the electrode and no vibration takes place. The prospect was experimentally ascertained at the several conditions of the applied voltage cited in Figure 3. Condition A corresponds to the dark discharge (applied voltage = 1 kV), B is the transition from the dark discharge to the corona discharge (3 kV), C is the stable corona discharge (5 kV), and D is just below the occurrence of spark discharge (6 kV). An experimental set-up to observe the vertical vibration of the pin electrode is common with Figure 1. The high stiffness plate was used as the support of the pin electrode. The laser displacement meter was used to measure the vertical vibration of the pin electrode and wave signals were recorded by a digital oscilloscope. Figure 4 shows the current and the vertical displacement of the pin electrode at the dark discharge A. The current was extremely small and the pin electrode did not vibrate as expected. However, at the transition B from the dark discharge to the corona discharge, corona current was unstable and it contained random pulse current as shown in Figure 5. Because the pulse current resulted in the pulse force, it caused vibration of the pin electrode. When the applied voltage was increased to the condition C, the corona current became stable again and therefore vibration did not take place but only the stable displacement of the pin electrode was observed as shown in Figure 6. The last case is shown in Figure 7 that the applied voltage was increased to D. Corona current was similar with that at the transition B, i.e., corona current was unstable and it contained random pulse current. Nevertheless no substantial vibration took place in this case, because major frequencies of the pulse did not coincide with the resonant frequency of the cantilever. Trichel pulse[7] also did not cause the electrode vibration because of the same reason at D. Frequency of the Trichel pulse is much higher than the natural frequency of the present system. Thus vibration of the softly supported pin electrode takes place at the condition that discharge current fluctuates and its frequency coincides with the natural frequency of the electrode.

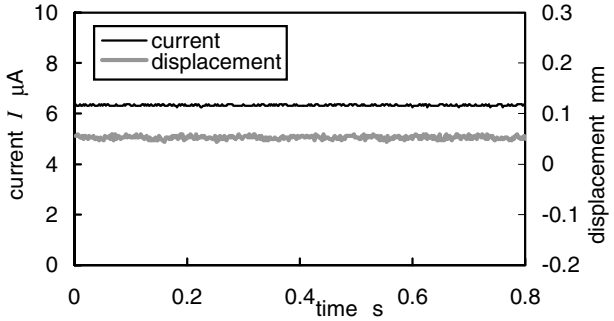

Figure 6. Vertical displacement of pin electrode and discharge current. (5 kV, positive, ϕ 0.5 mm pin diameter, 5 mm air gap)

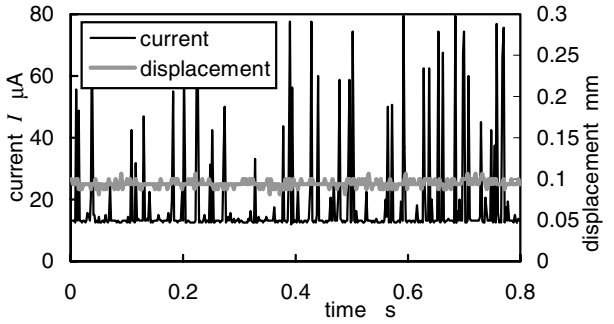

Figure 7. Vertical vibration of pin electrode and discharge current. (6 kV, positive, ϕ 0.5 mm pin diameter, 5 mm air gap)

Vibration of Pin Electrode at Spark Discharge

If the applied voltage increased at a certain value, spark discharge takes place and at the same time vertical vibration of the cantilever was induced as shown in Figures 8-11. The experimental set-up was also common with Figure 1. The high stiffness plate (stiffness 2.68 N/m, damping ratio 0.00179, natural frequency 9.79 Hz) was used as the support of the pin electrode. At the very beginning of the spark discharge, occurrence of the spark discharge was unstable and random. Although the occurrence of the spark was random, the cantilever began to vibrate in the vertical direction just at the start of the spark discharge. It is shown in Figure 8. If the applied voltage was increased, the spark discharge became periodic as shown in Figure 9. The vibration coupled with the occurrence of the spark discharge. The spark discharge took place almost when the pin electrode approached to the plate electrode. The amplitude of the vibration was large, in the order of 1 mm, which was about 10 times as large as the static displacement at the corona discharge. Pulse width of the spark discharge was 0.5-5 ms, which was short enough compared to a period of the free vibration. These experimental results suggested that the force at the spark discharge was *attractive* and its magnitude was much larger than the static repulsive force at the corona discharge. Comparison of the positive case in Figure 9 and the negative case in Figure 10 deduced that these characteristics were common at both positive and negative spark discharge. It is not clarified so far why such attractive force is induced at spark discharge. If the applied voltage further increased or the air gap was reduced, spark discharge took place independently on the displacement direction. The reason is that the spark condition was realized even when the pin electrode located at the upper point of the vibration. Because the spark frequency (~ 40 Hz) was much higher than the natural frequency of the electrode (~ 10 Hz), the amplitude of the forced vibration was small as shown in Figure 11. If the natural frequency of the electrode coincides with the spark frequency, resonant vibration will be induced.

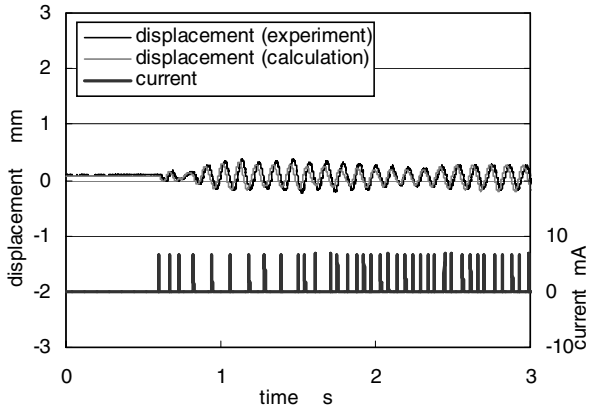

Figure 8. Vertical vibration of pin electrode and discharge current. (6.35 kV, positive, ϕ 0.5 mm pin diameter, 3 mm air gap)

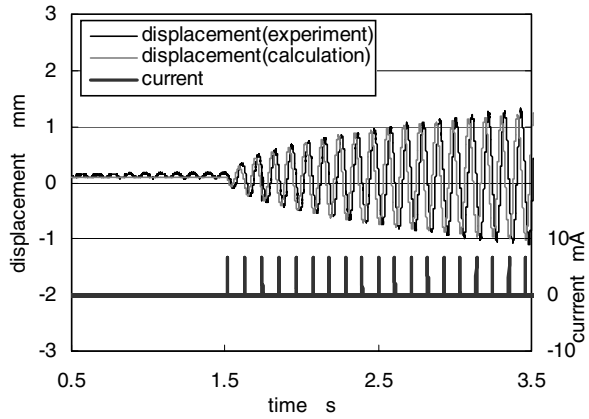

Figure 9. Vertical vibration of pin electrode and discharge current. (8.12 kV, positive, ϕ 0.5 mm pin diameter, 4 mm air gap)

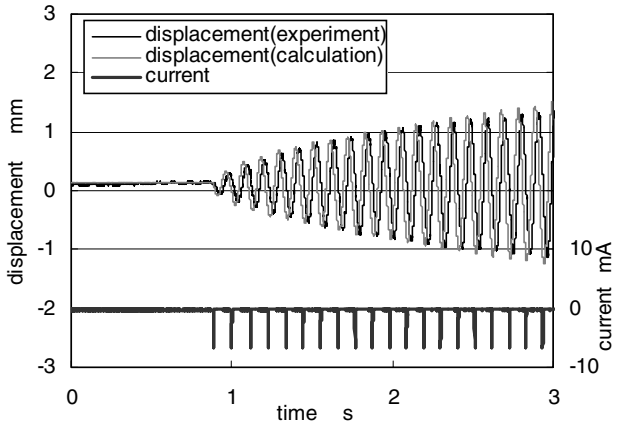

Figure 10. Vertical vibration of pin electrode and discharge current. (8.12 kV, negative, ϕ 0.5 mm pin diameter, 4 mm air gap)

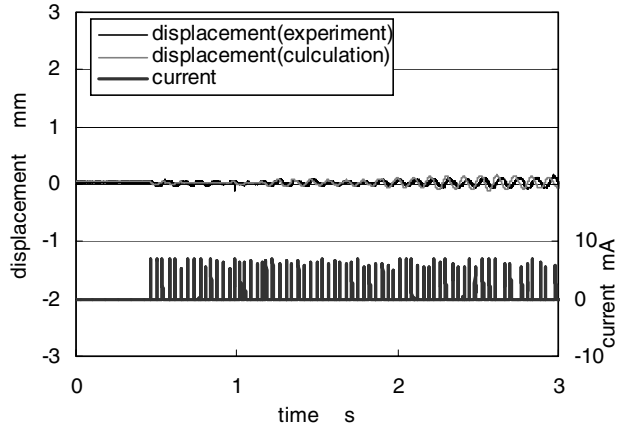

Figure 11. Vertical vibration of pin electrode and discharge current. (4.73 kV, positive, ϕ 0.5 mm pin diameter, 2 mm air gap)

The following explicit method was used to quantitatively evaluate the force at the spark discharge, for it was difficult to measure directly the small force at the short period of the spark discharge. The vibration of the cantilever connected to the pin electrode is simplified as the single-degree-of-freedom with respect to the vertical displacement z (upper direction is designated to be positive).

$$m\ddot{z} + c\dot{z} + kz = F(t) \quad ,$$

where m is an equivalent mass of the pin electrode and the cantilever, c is a viscous dumping coefficient, and k is the stiffness of the cantilever. These parameters were determined from a free vibration response. F is the vertical force acting on the pin electrode due to gas discharge. The force at corona discharge has already measured by the separate experiment[6] but the magnitude of the force at spark discharge had been unclear. It is determined explicitly, i.e., the numerical calculation is repeated with a revised force from an initial guess until the calculated vibration response coincides with the measured. The calculation is conducted using the Runge-Kutta method on the lumped-force assumption that the force at the spark discharge and that at the corona discharge are constant at each discharge period. It was proved that the method was adequate by the evidence that calculated results in Figures 8-11 agreed well with the measured. Figures 12 and 13 are derived forces at the spark discharge. It was elucidated that the force was attractive and the order of the magnitude was 1 mN. The force at the positive discharge was larger than that at the negative discharge. The force became large in accordance with the increase of the applied voltage, or the air gap, both in positive and negative discharge. Because the voltage of the spark discharge depended on the air gap, it is not clear so far that which factor, voltage or air gap, affects the force. Further investigation is necessary on the mechanism of the force generation itself.

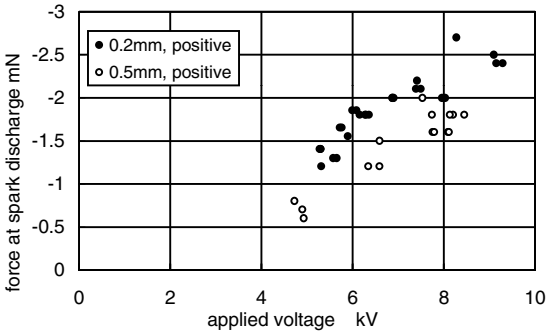

Figure 12. Electrostatic force applied to pin electrode at positive spark discharge.

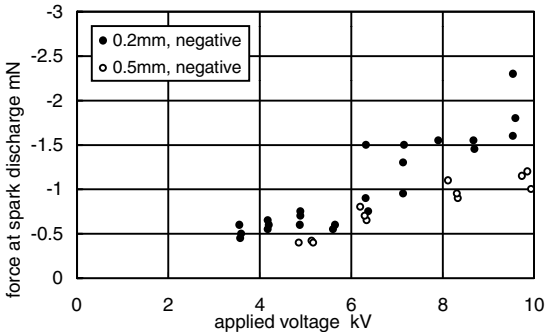

Figure 13. Electrostatic force applied to pin electrode at negative spark discharge.

Figures 14 and 15 are the frequency of the vibration measured by a FFT analyzer. It is recognized that the frequency at the corona discharge, designated in empty marks, equals to the natural frequency, while that at the spark discharge, solid marks, was a little smaller than the natural frequency. The decrease of the frequency at the positive discharge was smaller than that at the negative discharge.

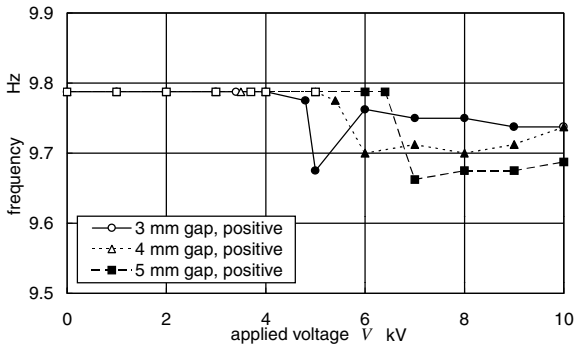

Figure 14. Frequency of free vibration and spark-discharge-coupled forced vibration. (positive, 0.5 mm pin diameter)

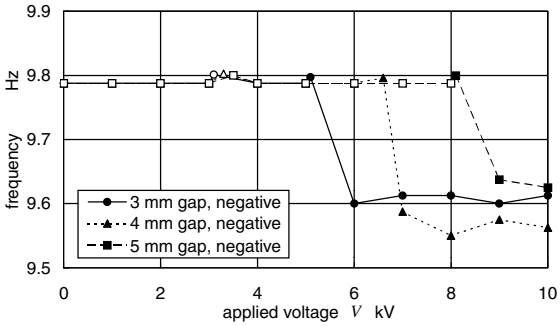

Figure 15. Frequency of free vibration and spark-discharge-coupled forced vibration. (negative, 0.5 mm pin diameter)

Electrostatic Ink Jet Phenomenon

A preliminary experiment was conducted on an electrostatic ink jet phenomenon. The experimental set-up is shown in Figure 16. An insulative capillary tube filled with water was used for the pin electrode. Because impurities were dissolved in water, water in the tube was electroconductive. If the tube diameter and/or water level were large, water leaked from the lower open end of the tube without the application of voltage. On the other hand, if these parameters were small, water leaked at any condition. The ink jet phenomenon was observed at the dark discharge under conditions of appropriate tube diameter and water level. Although the electrostatic attractive force is small, in the order of 10 μN at the voltage lower than the corona onset, it is large enough to separate a water droplet against surface tension in the capillary tube at certain conditions. At the corona discharging, however, water mist was dispersed from the tip of the tube.[8] Joule heat is assumed to be one of reasons of the mist generation. Details of these interesting phenomena are being investigated.

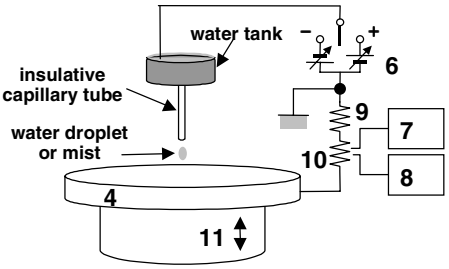

Figure 16. Experimental set-up to demonstrate electrostatic ink jet phenomenon.

Electrostatic Moses Effect

A preliminary experiment to visualize airflow near the electrodes suggested that ionic wind caused the repulsive force to the pin electrode at corona discharge. Pressure at the surface of the plate electrode was measured to confirm this hypothesis. Figure 17 shows an experimental set-up. A small hall, 0.2 mm in diameter, opened at the center of the plate electrode was introduced to a pressure gage (Nagano Keiki, GC62). The distance from the center of the pin electrode to the hole was adjusted by a xyz-stage. Some examples of measured results are shown in Figures 18-20 and Figure 21 is the force calculated by surface integral of the pressure. The force derived from the pressure integral agreed with the force measured by the static method at low voltage, but large discrepancy exists at high voltage. The reason is not clarified so far. It is also under investigation.

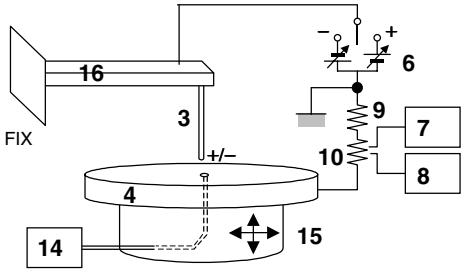

Figure 17. Experimental set-up to measure pressure at the surface of plate electrode. (14: pressure gage, 15: xyz-stage, 16: rigid support)

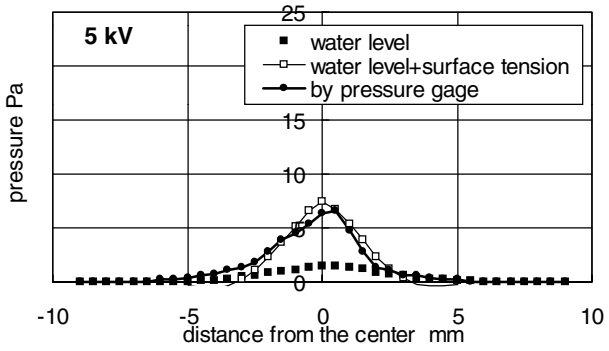

Figure 18. Radial distribution of pressure of corona wind at the surface of plate electrode and water level. (5 kV, positive, ϕ 0.5 mm pin diameter, 7 mm air gap)

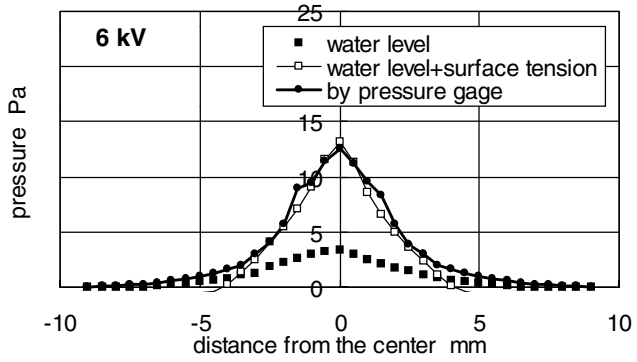

Figure 19. Radial distribution of pressure of corona wind at the surface of plate electrode and water level. (6 kV, positive, ϕ 0.5 mm pin diameter, 7 mm air gap)

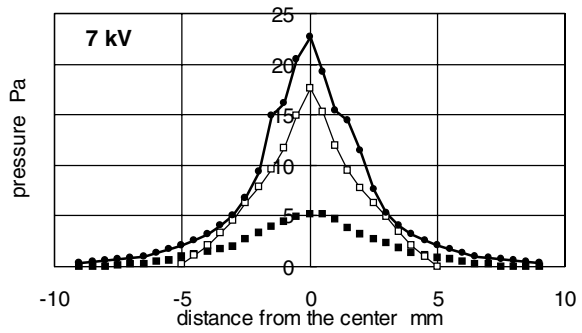

Figure 20. Radial distribution of pressure of corona wind at the surface of plate electrode and water level. (7 kV, positive, ϕ 0.5 mm pin diameter, 7 mm air gap)

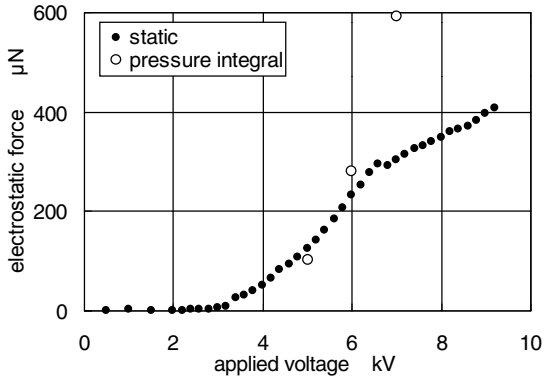

Figure 21. Force applied to pin electrode. (positive, ϕ 0.5 mm pin diameter, 7 mm air gap)

If the plate electrode made of metal is replaced to water, repulsive reaction force at corona discharge might change the shape of water level. This is confirmed by experiment using a set-up shown in Figure 22. If the applied voltage was lower than the corona onset threshold, change of water level was invisible to the naked eye. However, over the threshold voltage a relatively large repulsive force was induced and thus the water sank as shown in Figure 23. Change of water level was measured by the laser displacement meter (Keyence Corp., LK-080) that could be slid in the horizontal direction. Black ink was dissolved in water to enhance ionic conduction and to reflect the laser beam from the displacement meter. Some examples of measured results were added in Figures 18-20. One-millimeter change of water level equals to 10 Pa. Because the air gap became longer at corona discharge, actual air gaps at the center are designated in the figure captions to compare with the pressure distributions at the same air gap. The pressure derived by the change of the water level was smaller than the actual pressure measured by the pressure gage. Surface tension must be added to the water level to compare directly with the actual pressure distribution. It was calculated by the following method: (1) distribution of water level was fitted to the normal distribution, (2) radius of curvature was calculated, and (3) surface tension was calculated by Laplace law.[9] Here the measured coefficient of surface tension was used for calculations. It was almost the same with that of pure water, 72 mN/m. The distribution of the water level plus the calculated surface tension roughly agreed with the pressure distribution measured by the pressure gage, although water surface was no exactly flat. All of these evidences support the hypothesis that the ionic wind is the cause of repulsive force at corona discharge.

If the applied voltage further increased and the spark discharge took place, gravity wave of water was induced. We named these interesting static and dynamic phenomena "Electrostatic Moses Effect."

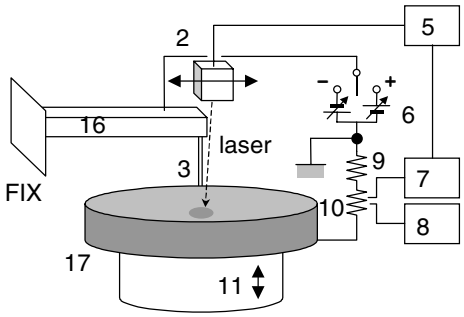

Figure 22. Experimental set-up to measure water level at corona discharge. (17: water tank)

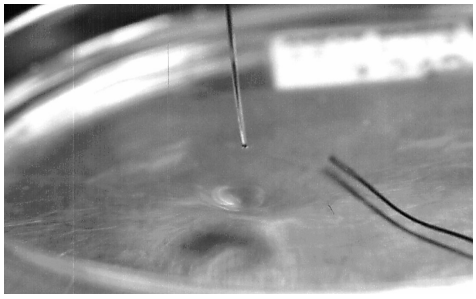

Figure 23. Electrostatic Moses effect. High voltage (~7 kV) is applied between the upper pin electrode (0.5 mm diameter) and the lower water as Moses stretched out his hand over the sea. (Exodus 14:21)

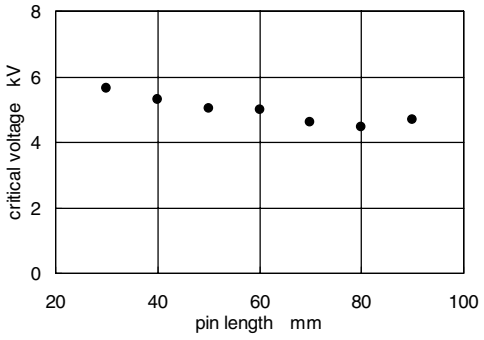

Figure 24. Critical voltage of corona jet phenomenon. (positive, ϕ 0.089 mm pin diameter, 5 mm air gap)

Electrostatic Air Jet Phenomenon

When the flexural rigidity of the pin electrode was extremely low, unstable vibration of the pin electrode, flutter, took place at corona discharge over a certain threshold voltage. We termed this interesting phenomenon "corona jet," for this is assumed to be aerodynamic instability due to the ionic wind. Figure 24 shows the relationship between the pin length and the threshold voltage. A series of investigation has been conducted on the kinetics of a wire-to-plate discharge system to clarify the mechanism of lateral oscillation that is sometimes observed in the corona charger used for a polyester film manufacturing machine.[10] It was reported that in the worst case the vibration caused breakdown of the wire, and then an effective countermeasure was proposed. On the other hand, to the author's knowledge, nothing has been reported on dynamic instability of the pin electrode in the pin-to-plate system. We have started the basic investigation on this phenomenon.

Concluding Remarks

Some interesting phenomena have been found and investigated on dynamics of a pin electrode in a pin-to-plate discharge system. These are; (1) vibration of the pin electrode at corona discharge due to fluctuation of corona current, (2) spark-coupled-vibration of the pin electrode at the non-selfsustaining spark discharge, (3) electrostatic ink jet phenomenon from the capillary tube, (4) electrostatic Moses effect for a water plate electrode, and (5) electrostatic flutter due to ionic wind.

It is expected that these phenomena be utilized for a new ozone free charger, a new ink jet system, improvement of the bead-carry-out in the two-component magnetic blush development subsystem of electrophotography, and also a new driving system of a micromachine.

Acknowledgement

The authors would like to express their thanks to N. Kumagai (Ricoh Co.), S. Umezu, K. Arai, K. Watanabe, N. Murata, J. Shiraishi, R. Koizumi, F. Sasamoto, and Y. Kawabe (Waseda Univ.) for their help of carrying out experiments. This work is supported by Grant-in-Aid for Scientific Research (No. 12650235) of the Japan Society for Promotion of Science.

References

1. T. B. Hansen and B. Andersen, *Am. Ind. Hyg. Assoc. J*, **47**, 659 (1986).
2. K. Furukawa, H. Ishii, K. Shiojima and T. Ishikawa, Proc. *IS&T's Tenth Int. Congress on Advances in Non-Impact Printing Technologies*, 34 (1994).
3. K. Furukawa, H. Ishii, K. Shiojima and T. Ishikawa, *Electrophoto*, **35**, 116 (1996).
4. H. Kawamoto, *J. Imaging Sci. Technol*, **44**, 452 (2000).
5. E. M. Williams, *The Physics and Technology of Xerographic Processes*, Krieger Publishing Co., Malabar, FL, 1992.
6. H. Kawamoto, K. Takasaki, H. Yasuda and N. Kumagai, *IS&T's NIP16: International Conference on Digital Printing Technologies*, Vancouver, 827 (2000).
7. W. L. Lama and C. F. Gallo, *J. Appl. Phys*, **45**, 103 (1974).
8. J-D. Moon, J-G. Kim and D-H. Lee, *IEEE Trans. on Industry Applications*, **34**, 1212 (1998).
9. L. D. Landau and E. M. Lifshitz, "Fluid Dynamics," Pergamon Press, Oxford (1960).
10. Y. Ito, Dynamics of the Wire Electrode in a System of Wire and Plate Electrodes, Ph.D. Thesis, Keio University (1996).

Biography

KAWAMOTO, Hiroyuki holds a BS degree in Electrical Engineering from Hiroshima Univ. (1972) and a Dr. degree in Mechanical Engineering from Tokyo Institute of Technology (1983). From 1972 to 1991 he was a Senior Engineer at the Nuclear Division of Hitachi Ltd. In 1991 he moved to Fuji Xerox, and had been engaged in the research of electrophotography as a Research Fellow. In 1999 he left Fuji Xerox and he is now a professor of Waseda Univ. His awards include the Japan Society of Mechanical Engineers Young Scientist Award (1984), the 7th International Microelectronics Conf. Best Paper Award (1992), the Japan Institute of Invention and Innovation Patent Award (1993), and the 10th International Symposium on Applied Electromagnetics and Mechanics, Award for Outstanding Presentation Paper (2001). He was selected a Fellow of the IS&T in 1999.